ARTICLE IN PRESS

Available online at www.sciencedirect.com

SCIENCE DIRECT

ELSEVIER

Journal of Computational and Applied Mathematics ▮▮▮ (▮▮▮▮) ▮▮▮–▮▮▮

JOURNAL OF COMPUTATIONAL AND APPLIED MATHEMATICS

www.elsevier.com/locate/cam

High-order discretization and multigrid solution of elliptic nonlinear constrained optimal control problems

A. Borzì

Institut für Mathematik und Wissenschaftliches Rechnen, Karl-Franzens-Universität Graz, Heinrichstr. 36, A-8010 Graz, Austria

Received 29 June 2005; received in revised form 13 December 2005

Abstract

High(-mixed)-order finite difference discretization of optimality systems arising from elliptic nonlinear constrained optimal control problems are discussed. For the solution of these systems, an efficient and robust multigrid algorithm is presented. Theoretical and experimental results show the advantages of higher-order discretization and demonstrate that the proposed multigrid scheme is able to solve efficiently constrained optimal control problems also in the limit case of bang-bang control.

MSC: 49K20; 65N06; 65N12; 65N55

Keywords: Optimal control problems; Optimality systems; Finite differences; Multigrid methods

1. Introduction

Recent theoretical and experimental results give evidence that multigrid methods allow to solve elliptic optimal control problems with optimal computational complexity and are robust with respect to changes of values of the optimization parameters; see, e.g. [2–5,10,13,27]. These results refer to multigrid methods applied to second-order discretizations of elliptic optimality systems. Less is known on higher-order discretization of optimality systems and their solution by multigrid methods.

Concerning discretization, in the case of optimal control problems without constraints on the control, second-order discretization results in second-order accurate optimal solutions; see [3,4] for the case of finite differences discretization and [1,21] for the case of finite element discretization. Further, in [4,25] it is shown that, in the presence of constraints on the control, second-order discretization results also in second-order accurate solution for the state variable and $\frac{3}{2}$-accurate solution of the control. However, in this case special techniques [17,22] are available that allow to recover second-order accurate optimal controls.

In this paper, higher-order finite differences discretization of optimality systems are defined to approximate unconstrained and constrained nonlinear optimal control problems. Based on the so-called first optimize then discretize approach, we first derive the first-order optimality conditions for a minimum in a continuous setting and then discretize the resulting coupled differential system by using a second-order or a higher fourth-order discretization scheme. The advantage of this approach is the possibility of choosing different order of discretization for the different equations defining the optimality system, allowing to investigate the influence of the accuracy of the state and of the adjoint

E-mail address: alfio.borzi@uni-graz.at.

0377-0427/$ - see front matter © 2006 Elsevier B.V. All rights reserved.
doi:10.1016/j.cam.2005.12.023

variables on the overall accuracy of the optimal solution. Notice that choosing the same discretization scheme for the state and adjoint equations corresponds also, in our case, to the first discretize and then optimize approach. While we do not address adaptivity in this paper, we think that this study may provide a contribution to the research on adaptivity for constrained optimal control problems. In fact, it gives insight on the dependence of the accuracy of optimal solutions on the degree of approximation of the state equation as opposed to that of the adjoint equation, suggesting that adaptivity should be driven by errors related to the state equation.

Motivated by the need of solving optimality systems discretized by mixed-order schemes and by previous successful applications, we discuss the development and analysis of a multigrid method for the optimality systems mentioned above. The multigrid method proposed in this paper is of the full-approximation-storage (FAS) type and uses a smoothing iteration resulting from our previous experience on multigrid methods for singular [3] and constrained [4] optimal control problems, and from the theoretical investigation presented in [5]. This smoothing procedure appears to be robust with respect to changes of the value of the optimization parameter allowing, in particular, to investigate bang-bang type control phenomena [11]. The resulting multigrid scheme shows typical mesh-independent convergence factors.

The main results presented in this paper are: (1) An a priori accuracy estimate for higher-order finite difference discretization of linear optimality systems for the unconstrained case; (2) Development of a multigrid algorithm for a class of higher-order finite differences optimality systems; (3) Formulation of a smoothing iteration for nonlinear control-constrained optimal control problems; (4) Twogrid Fourier analysis of convergence of the proposed multigrid solver; (5) Numerical investigation of the influence of mixed higher-order schemes on the optimal solution.

For the discussion that follows, we introduce a nonlinear optimal control problem with constrained distributed control in Section 2. For detailed guidelines of how to extend the present approach to the case of boundary control problems see [4]. In Section 3, accuracy of finite differences approximation to solutions of optimal control problems is discussed considering a linear model. For the discretization of the elliptic operator, the standard five-point and a nine-point stencils are chosen. Correspondingly, optimal accuracy estimates are obtained. In Section 5, a nonlinear multigrid scheme is formulated. The nonlinear approach is appropriate because of the presence of nonlinearity and suitable in order to implement the inequality constraint at all levels of the multigrid process. The main effort in the development of the present solver is in the construction of a relaxation scheme which satisfies the constraints imposed on the control function. Because of the constraints, the optimality condition is not differentiable in the classical sense and a smoother based on local Newton steps as in [3] cannot be defined. For this reason, we present an alternative approach which avoids differentiation of the optimality condition. In Section 6, for a linear model and without constraints, we obtain sharp convergence factor estimates for the multigrid scheme applied to optimality systems discretized by mixed-order schemes.

Results of numerical experiments are reported in Section 7 that demonstrate the ability of our algorithm to solve constrained optimal control problems also in the limit case of bang-bang control. Further results give evidence that higher-order approximation of the state equation is more advantageous than higher-order approximation of the adjoint equation. In particular, we show that fourth-order optimal solutions, including the control function, can be obtained even when the constraints are active. A section of conclusions completes this exposition.

2. Nonlinear constrained optimal control problems

As a model problem for our investigation we consider a material plate defining a two-dimensional convex domain Ω. For the state y of the material we choose the temperature distribution which is maintained equal to zero along the boundary. We assume thermal radiation or positive temperature feedback due to chemical reactions represented by the term $G(y)$; see, e.g. [23]. For later convenience we let the presence of a source f defined on Ω. This system is governed by the following equation:

$$\begin{cases} \Delta y + G(y) = f & \text{in } \Omega, \\ y = 0 & \text{on } \partial\Omega. \end{cases} \tag{1}$$

In particular, we consider nonlinearity of the form $G(y) = \sigma\, y^q$. In the case $\sigma < 0$ and $q = 4$ the nonlinear term represents the Stefan–Boltzmann law of radiation emitting from the surface of the plate. The case $\sigma > 0$ and $q > 1$, describes positive energy production and the corresponding problem (1) is not coercive and may not admit solutions, similarly to the problem discussed in [3]. The latter case is more challenging and for the numerical experiments we

choose $\sigma = 1$ and $q = 4$. Results of numerical experiments demonstrate that coercivity of the state equation is not essential in our multigrid approach.

The setting above suggests that we may control the temperature distribution y to come close to a given target profile $z \in L^2(\Omega)$ by acting with an additional distributed source term u, the control function. The corresponding optimal control problem is formulated as follows:

$$\begin{cases} \min_{u \in U_{\mathrm{ad}}} J(y, u) \\ \Delta y + G(y) = u + f & \text{in } \Omega, \\ y = 0 & \text{on } \partial\Omega, \end{cases} \tag{2}$$

where we assume that $u \in U_{\mathrm{ad}}$, $U_{\mathrm{ad}} \subset L^2(\Omega)$ being the set of admissible controls given by

$$U_{\mathrm{ad}} = \{u \in L^2(\Omega) \mid \underline{u}(\mathbf{x}) \leqslant u(\mathbf{x}) \leqslant \overline{u}(\mathbf{x}) \quad \text{a.e. in } \Omega\}, \tag{3}$$

where $\underline{u}$ and $\overline{u}$ are elements of $L^\infty(\Omega)$. For the formulation of optimal control problems where the control acts only in a part of the whole domain see [4].

The cost functional J is of the tracking type and is given by

$$J(y, u) = \frac{1}{2}\|y - z\|^2_{L^2(\Omega)} + \frac{\nu}{2}\|u\|^2_{L^2(\Omega)}, \tag{4}$$

where $\nu \geqslant 0$ is the weight of the cost of the control.

Existence of solutions to (2)–(4) can be established under suitable conditions for various forms of the nonlinearity; see, e.g. [3,12,20]. Take $G \in C^\infty$ monotonically decreasing function with $G(0) = 0$. Results for singular optimal control problems can be found in, e.g., [18,20].

Optimal solutions are characterized by the following optimality system

$$\begin{aligned} &\Delta y + G(y) = u + f && \text{in } \Omega, \\ &y = 0 && \text{on } \partial\Omega, \\ &\Delta p + G'(y)\, p = -(y - z) && \text{in } \Omega, \\ &p = 0 && \text{on } \partial\Omega, \\ &(\nu u - p,\ v - u) \geqslant 0 && \text{for all } v \in U_{\mathrm{ad}}. \end{aligned} \tag{5}$$

We refer to the first differential equation of (5) as the state equation and to the second one as the adjoint equation. Notice that the last equation in (5) giving the optimality condition is equivalent to (see [19])

$$u = \max\left\{\underline{u}, \min\left\{\overline{u}, \frac{1}{\nu}p(u)\right\}\right\} \quad \text{in } \Omega, \quad \nu > 0. \tag{6}$$

The nondifferentiability of this equation prevents the use of the classical Newton approach, requiring more sophisticated techniques [16,24] based on a generalized differentiability concept. In Section 5, we follow an alternative approach where differentiation of (6) is not required.

We complete this section recalling that the solution to (2)–(4) with $\nu = 0$ is characterized by the following differential system:

$$\begin{aligned} &\Delta y + G(y) = u + g && \text{in } \Omega, \\ &y = 0 && \text{on } \partial\Omega, \\ &\Delta p + G'(y)\, p = -(y - z) && \text{in } \Omega, \\ &p = 0 && \text{on } \partial\Omega, \\ &p = \min\{0, p + u - \underline{u}\} + \max\{0, p + u - \overline{u}\} && \text{in } \Omega. \end{aligned} \tag{7}$$

3. High-order finite difference discretization

While linear finite element approximations [1,21,22,25] and second-order finite difference approximations [3–5] have been previously investigated, much less is known for higher-order discretization of optimality systems. In this section we discuss higher-order finite differences discretization for a linear optimality system with $\nu > 0$ and no constraints.

Consider a sequence of grids $\{\Omega_h\}_{h>0}$ given by

$$\Omega_h = \{\mathbf{x} \in \mathbf{R}^2 : x_i = s_i\, h, \quad s_i \in \mathbb{Z}\} \cap \Omega.$$

We assume that Ω is a rectangular domain and that the values of the mesh size h are chosen such that the boundaries of Ω coincide with grid lines. For grid functions v_h and w_h defined on Ω_h we introduce the discrete L^2-scalar product

$$(v_h, w_h)_{L_h^2} = h^2 \sum_{\mathbf{x}\in\Omega_h} v_h(\mathbf{x})\, w_h(\mathbf{x}),$$

with associated norm $|v_h|_0 = (v_h, v_h)_{L_h^2}^{1/2}$. We also need $|v_h|_\infty = \max_{\mathbf{x}\in\Omega_h} |v_h(\mathbf{x})|$.

First-order backward and forward partial derivatives of v_h in the x_i direction are denoted by ∂_i^- and ∂_i^+, respectively, and given by

$$\partial_i^- v_h(\mathbf{x}) = \frac{v_h(\mathbf{x}) - v_h(\mathbf{x} - \hat{\imath}\, h)}{h} \quad \text{and} \quad \partial_i^+ v_h(\mathbf{x}) = \frac{v_h(\mathbf{x} + \hat{\imath}\, h) - v_h(\mathbf{x})}{h},$$

where $\hat{\imath}$ denotes the i coordinate direction vector and v_h is extended by 0 on grid points outside of Ω; see [15]. In this framework, the discrete H^1-product is given by

$$|v_h|_1 = \left(|v_h|_0^2 + \sum_{i=1}^{2} |\partial_i^- v_h|_0^2 \right)^{1/2}.$$

The spaces L_h^2 and H_h^1 consist of the sets of grid functions v_h endowed with $|v_h|_0$, respectively, $|v_h|_1$, as norm. We need the following lemma [28].

Lemma 1 (*Poincaré–Friedrichs inequality for finite differences*). *For any grid function v_h, there exists a constant c_*, independent of v_h and h, such that*

$$|v_h|_0^2 \leqslant c_* \sum_{i=1}^{2} |\partial_i^- v_h|_0^2. \tag{8}$$

(Note: for $\Omega = (0, 1) \times (0, 1)$, $c_* = \frac{1}{4}$.)

Functions in $L^2(\Omega)$ and $H^1(\Omega)$ are approximated by grid functions defined through their mean values with respect to elementary cells $[x_1 - h/2, x_1 + h/2] \times [x_2 - h/2, x_2 + h/2]$; see [15] for more details. For sufficiently smooth functions $v \in C^k(\bar{\Omega})$ (resp. $f \in C^k(\Omega)$), $k = 0, 1, \ldots$, we denote with $(R_h v)(x) = v(x)$ (resp. $(\tilde{R}_h f)(x) = f(x)$) the restriction operator on $\bar{\Omega}_h$ (resp. Ω_h).

The (standard) second-order five-point approximation to the Laplacian with homogeneous Dirichlet boundary conditions is defined by

$$\tilde{\Delta}_h = \partial_1^+ \partial_1^- + \partial_2^+ \partial_2^-.$$

We have the following consistency result

$$|\tilde{\Delta}_h R_h v - \tilde{R}_h \Delta v|_\infty \leqslant c\, h^2 \|v\|_{C^4(\bar{\Omega})}, \tag{9}$$

see, e.g. [15].

As mentioned in [15], the five-point formula above is optimal in the sense that there is no compact nine-point formula which provides an order of accuracy higher than two. Indeed, Collatz's compact nine-point scheme provides

fourth-order accuracy when used in combination with a five-point representation of the right-hand side. In the case of optimality systems the use of the compact nine-point scheme requires a five-point representation of the control $u \in C^2(\Omega)$ in the state equation and of y in the adjoint equation. However, we can show that in cases where constraints are active, the control u may result not sufficiently smooth to allow Collatz's approach and in these cases the accuracy of the compact nine-point optimal control solution collapses to second order. For this reason, we use the extended nine-point schema considered in [6,26] which is suitable for less smooth controls. We have the following fourth-order nine-point approximation to the Laplacian

$$\Delta_h = \left(1 - \frac{h^2}{12}\partial_1^+\partial_1^-\right)\partial_1^+\partial_1^- + \left(1 - \frac{h^2}{12}\partial_2^+\partial_2^-\right)\partial_2^+\partial_2^-. \tag{10}$$

For more insight, the one-dimensional expanded form of this operator is given by

$$\left(1 - \frac{h^2}{12}\partial_1^+\partial_1^-\right)\partial_1^+\partial_1^- v(x) = \frac{1}{12h^2}(-v(x-2h) + 16\,v(x-h) - 30\,v(x) + 16\,v(x+h) - v(x+2h)).$$

At grid points with distance h from the boundary, the operator Δ_h must be modified. In [6] it is shown that the approximation of the Laplacian near the boundary need be only $\mathcal{O}(h^2)$ without destroying the overall fourth-order accuracy of the scheme. Thus the five-point $\tilde{\Delta}_h$ operator could be used (in particular to implement boundary controls as in [4]). However, on coarse grids we find that the following asymmetric fourth-order approximation of the second partial derivative is more accurate. For $\mathbf{x} \in \Omega_h$ next to the left-hand side boundary we have [26]

$$\frac{\partial^2 v}{\partial x_1^2} \approx \frac{1}{12h^2}\,(10\,v(x_1 - h) - 15\,v(x_1) - 4\,v(x_1 + h) + 14\,v(x_1 + 2h) - 6\,v(x_1 + 3h) + v(x_1 + 4h)). \tag{11}$$

Schemes (10) and (11) result in a matrix of coefficients which is neither diagonally dominant nor of non-negative type [6]. Nevertheless, in the case that $\tilde{\Delta}_h$ is used close to the boundary, it is proved in [6] that the resulting problem satisfies a maximum principle. The same proof applies with few modifications to the case when (11) is used instead (change the second row of the matrix A in (2.6) of [6] and verify that the required property for AG in (2.15) of [6] holds). Further we have that

$$|\Delta_h R_h v - \tilde{R}_h \Delta v|_\infty \leqslant c\,h^4 \|v\|_{C^6(\bar{\Omega})}, \tag{12}$$

where c is independent of v and h.

Next, an a priori estimate of the accuracy of solutions to a linearized version of the optimality system (5) without constraints on the control is discussed. Set $G(y) = gy$ with $g \leqslant 0$ and $U_{\mathrm{ad}} = L^2(\Omega)$. The last equation in (5) then becomes $vu - p = 0$, which we can use in the first equation of the system to eliminate the control variable u. After discretization we have the following discrete optimality system:

$$\Delta_h y_h + g\,y_h - p_h/v = \tilde{f}_h, \tag{13}$$
$$\Delta_h p_h + g\,p_h + y_h = \tilde{z}_h, \tag{14}$$

where $\tilde{f}_h = \tilde{R}_h f$ and $\tilde{z}_h = \tilde{R}_h z$.

Now consider the inner product of (13) by $v\,y_h$ and of (14) by p_h and take the sum of the two resulting equations. We obtain

$$v\,(\Delta_h y_h, y_h)_{L_h^2} + (\Delta_h p_h, p_h)_{L_h^2} + v\,g\,|y_h|_0^2 + g\,|p_h|_0^2 = v\,(\tilde{f}_h, y_h)_{L_h^2} + (\tilde{z}_h, p_h)_{L_h^2},$$

which implies that

$$v\,(-\Delta_h y_h, y_h)_{L_h^2} + (-\Delta_h p_h, p_h)_{L_h^2} - v\,g\,|y_h|_0^2 - g\,|p_h|_0^2 \leqslant v\,|(\tilde{f}_h, y_h)_{L_h^2}| + |(\tilde{z}_h, p_h)_{L_h^2}|.$$

By construction (10), we have that $(-\Delta_h v_h, v_h)_{L_h^2} \geqslant (-\tilde{\Delta}_h v_h, v_h)_{L_h^2}$ for all functions v_h. Because $(-\tilde{\Delta}_h v_h, v_h)_{L_h^2} = \sum_{i=1}^2 |\partial_i^- v_h|_0^2$ and using Lemma 1, we obtain

$$v\,(1 + c_*|g|)\,|y_h|_0^2 + (1 + c_*|g|)\,|p_h|_0^2 \leqslant c_*\,v\,|(\tilde{f}_h, y_h)_{L_h^2}| + c_*\,|(\tilde{z}_h, p_h)_{L_h^2}|.$$

Applying the Cauchy–Schwarz and Cauchy inequalities on the right-hand side of this expression results in

$$\nu\,|y_h|_0^2 + |p_h|_0^2 \leqslant c\,(\nu\,|\tilde{f}_h|_0^2 + |\tilde{z}_h|_0^2), \tag{15}$$

where $c = c_*/(2(1 + c_*|g|) - c_*)$. We remark that the same inequality is obtained if we use $\tilde{\Delta}_h$ in place of Δ_h in (13) and/or (14).

Using (15), we are now able to determine the degree of accuracy of the optimal solution. For this purpose, notice that (13)–(14) hold true with y_h and p_h replaced by their respective error functions, and with $\tilde{f}_h$ and $\tilde{z}_h$ replaced by the truncation error for Δ_h (resp. $\tilde{\Delta}_h$) estimated by (12) (resp. by (9)). Further notice that dividing (15) by ν and recalling that $u_h = p_h/\nu$, we obtain the estimate for the control from $|y_h|_0^2 + \nu\,|u_h|_0^2 \leqslant c\,(|\tilde{f}_h|_0^2 + |\tilde{z}_h|_0^2/\nu)$. These statements are summarized in the following theorem.

Theorem 1. *Let* $y \in C^{k+2}(\bar{\Omega})$, $k = 2, 4$, *and* $p \in C^{l+2}(\bar{\Omega})$, $l = 2, 4$, *be solutions to* (5) (*with* $G = gy$, $g \leqslant 0$, *and no constraints on the control*), *and let* y_h *and* p_h *be solutions to* (13) and (14). *Then there exists a constant* c, *depending on* Ω, *and independent of* h, *such that*

$$|y_h - R_h y|_0^2 + \frac{1}{\nu}\,|p_h - R_h p|_0^2 \leqslant c\,\left(h^{2k}\,\|y\|^2_{C^{k+2}(\bar{\Omega})} + h^{2l}\,\frac{1}{\nu}\,\|p\|^2_{C^{l+2}(\bar{\Omega})}\right).$$

This estimate holds for linear optimality systems in the unconstrained case. Results of numerical experiments demonstrate its validity in the case of unconstrained optimal control problems with elliptic semilinear equations as governing equations. Unexpectedly, we obtain results of computation that give evidence that the estimate above may hold also in the case of controls with active constraints; see Section 7.

Extension of the results stated in Theorem 1 to nonlinear constrained optimal control problems appears difficult and unsatisfactory especially in the finite-difference framework. The analysis presented in [4] can be extended to the present setting obtaining first-order accuracy estimate for the control with constraints. The lack of a Aubin–Nitsche duality argument for finite differences prevents improvement of these estimates as it is possible in a finite element context.

4. Smoothing iteration for nonlinear constrained optimal control problems

In this and the following section we discuss a multigrid approach to the solution of the optimality system (5) with the discretization given above. A multigrid scheme combines two solution strategies: An iterative (smoothing) scheme (like Jacobi or Gauss–Seidel) that is effective in reducing high-frequency components of the solution error and a coarse-grid correction method that is efficient in solving the low-frequency error components. In this section we formulate our iterative scheme for the most general setting considered in this paper. The smoothing property of this scheme is discussed in Section 6.

Let $\mathbf{x} \in \Omega_h$, where $\mathbf{x} = (ih, jh)$ and i, j index the grid points, e.g., lexicographically. Denote with ω_{ij} the set of grid index pairs s, t of the stencil of Δ_h (resp. $\tilde{\Delta}_h$) centered at i, j. (For example, for $\tilde{\Delta}_h$ at $0, 0$ we have $\omega_{ij} = \{0, 0; 1, 0; -1, 0; 0, 1; 0, -1\}$.) Correspondingly, denote with c_{st} (resp. $\tilde{c}_{st}$), $s, t \in \omega_{ij}$, the s, t coefficient of the stencil (multiplied by h^2) centered at i, j. (In the example we have $c_{00} = -4$, $c_{10} = 1$, etc.) Using this notation, we can express the action of Δ_h (resp. $\tilde{\Delta}_h$) on the function v_h in the following compact form:

$$\Delta_h v_h|_{ij} = \frac{1}{h^2}\left(\sum_{s,t\in\omega_{ij},\, s,t\neq i,j} c_{st}\, v_{st} - c_{ij} v_{ij}\right).$$

Consider (32) and (33) at $\mathbf{x}$, we have

$$\sum_{s,t\in\omega_{ij},\, s,t\neq i,j} c^y_{st}\, y_{st} - c^y_{ij}\, y_{ij} + h^2\, G(y_{ij}) - h^2\, u_{ij} = h^2\, \tilde{f}_{ij}, \tag{16}$$

$$\sum_{s,t\in\omega_{ij},\, s,t\neq i,j} c^p_{st}\, p_{st} - c^p_{ij}\, p_{ij} + h^2\, G'(y_{ij})\, p_{ij} + h^2\, y_{ij} = h^2\, \tilde{z}_{ij}, \tag{17}$$

$$(\nu u_{ij} - p_{ij}) \cdot (v_{ij} - u_{ij}) \geqslant 0 \quad \text{for all } v_h \in U_{\mathrm{ad}h}, \tag{18}$$

where $U_{adh}=\{u \in L_h^2(\Omega_h) \mid \underline{u}(\mathbf{x}) \leqslant u(\mathbf{x}) \leqslant \overline{u}(\mathbf{x}) \text{ in } \Omega_h\}$ and $\tilde{f}$ and $\tilde{z}$ represent f_h and z_h including the defect corrections, discussed later in (35) and (36). Notice that for convenience we distinguish between the coefficient c_{st} for the y and p variables by writing c_{st}^y and c_{st}^p, respectively.

To ease notation we set

$$A_{ij} = \sum_{s,t\in\omega_{ij},\, s,t\neq i,j} c_{st}^y\, y_{st} - h^2 \tilde{f}_{ij} \quad \text{and} \quad B_{ij} = \sum_{s,t\in\omega_{ij},\, s,t\neq i,j} c_{st}^p\, p_{st} - h^2 \tilde{z}_{ij}.$$

Here A_{ij} and B_{ij} are considered constant during the update of the variables at i, j. Summarizing, we have the following system for the three scalar variables y_{ij}, p_{ij}, and u_{ij}:

$$A_{ij} - c_{ij}^y\, y_{ij} + h^2\, G(y_{ij}) - h^2\, u_{ij} = 0, \tag{19}$$

$$B_{ij} - c_{ij}^p\, p_{ij} + h^2\, G'(y_{ij})\, p_{ij} + h^2\, y_{ij} = 0, \tag{20}$$

$$(v u_{ij} - p_{ij}) \cdot (v_{ij} - u_{ij}) \geqslant 0 \quad \text{for all } v_h \in U_{adh}. \tag{21}$$

In the linear case and no constraints on the control, this system can be solved immediately and its solution gives an update to y_{ij}, p_{ij}, and u_{ij} defining a collective (all-at-once) Gauss–Seidel step as in [5]. In the nonlinear case without constraints, the solution of the system above is replaced by a local Newton update as in [3]. When constraints are present, the direct application of a classical Newton scheme is not possible because of the presence of the inequality constraint. In the following, we discuss another approach generalizing ideas in [4] that avoids differentiation of (21).

First, consider (19)–(20). The inverse of the Jacobian of these two equations is given by

$$J_{ij}^{-1} = \frac{1}{\det J_{ij}} \begin{pmatrix} -c_{ij}^p + h^2 G'(y_{ij}) & 0 \\ -h^2(1 + G''(y_{ij})\, p_{ij}) & -c_{ij}^y + h^2 G'(y_{ij}) \end{pmatrix}, \tag{22}$$

where $\det J_{ij} = (-c_{ij}^y + h^2 G'(y_{ij}))(-c_{ij}^p + h^2 G'(y_{ij}))$. Notice that h can be chosen sufficiently small to guarantee that $\det J_{ij} \neq 0$. Also notice that second-order necessary conditions for a minimum require that $(1 + G''(y_{ij})\, p_{ij}) \geqslant 0$.

For given u_{ij}, a local Newton update for the state and the adjoint variables $\hat{y}_{ij}$ and $\hat{p}_{ij}$ at i, j is given by

$$\begin{pmatrix} \hat{y}_{ij} \\ \hat{p}_{ij} \end{pmatrix} = \begin{pmatrix} y_{ij} \\ p_{ij} \end{pmatrix} + J_{ij}^{-1} \begin{pmatrix} r_{ij}^y \\ r_{ij}^p \end{pmatrix}, \tag{23}$$

where $r_{ij}^y = -(A_{ij} - c_{ij}^y\, y_{ij} + h^2\, G(y_{ij}) - h^2\, u_{ij})$ and $r_{ij}^p = -(B_{ij} - c_{ij}^p\, p_{ij} + h^2\, G'(y_{ij})\, p_{ij} + h^2\, y_{ij})$ denote the residual of (19) and (20), respectively. Notice that r_{ij}^y depends explicitly on u_{ij}. This fact allows us to write $\hat{p}_{ij}$ as a function of u_{ij} as follows:

$$\begin{aligned} \hat{p}_{ij}(u_{ij}) = p_{ij} &+ \frac{1}{\det\, J_{ij}} \left(h^2(1 + G''(y_{ij})\, p_{ij})\, (A_{ij} - c_{ij}^y\, y_{ij} + h^2\, G(y_{ij}))\right) \\ &+ \frac{1}{\det\, J_{ij}} \left((c_{ij}^y - h^2 G'(y_{ij}))\, (B_{ij} - c_{ij}^p\, p_{ij} + h^2\, G'(y_{ij})\, p_{ij} + h^2\, y_{ij})\right). \\ &- \frac{1}{\det\, J_{ij}} (1 + G''(y_{ij})\, p_{ij})\, h^4\, u_{ij}. \end{aligned} \tag{24}$$

Now to obtain first the update for u_{ij}, replace $\hat{p}_{ij}$ in the inequality constraint. From $v\tilde{u} - \hat{p}(\tilde{u}) = 0$ at i, j, we have the auxiliary variable

$$\begin{aligned} \tilde{u}_{ij} = &\left(v + \frac{(1 + G''(y_{ij})\, p_{ij})\, h^4}{\det\, J_{ij}}\right)^{-1} \\ &\times \left[p_{ij} + \frac{1}{\det\, J_{ij}} \left(h^2(1 + G''(y_{ij})\, p_{ij})\, (A_{ij} - c_{ij}^y\, y_{ij} + h^2\, G(y_{ij}))\right)\right. \\ &\left. + \frac{1}{\det\, J_{ij}} \left((c_{ij}^y - h^2 G'(y_{ij}))\, (B_{ij} - c_{ij}^p\, p_{ij} + h^2\, G'(y_{ij})\, p_{ij} + h^2\, y_{ij})\right)\right]. \end{aligned}$$

Then, the new value for u_{ij} resulting from the relaxation step is given by

$$u_{ij} = \begin{cases} \overline{u}_{ij} & \text{if } \tilde{u}_{ij} \geqslant \overline{u}_{ij}, \\ \tilde{u}_{ij} & \text{if } \underline{u}_{ij} < \tilde{u}_{ij} < \overline{u}_{ij}, \\ \underline{u}_{ij} & \text{if } \tilde{u}_{ij} \leqslant \underline{u}_{ij}. \end{cases} \tag{25}$$

With u_{ij} given, we can use (23) to obtain new values for y_{ij} and p_{ij}. This completes the description of the iteration step.

This step satisfies the inequality constraints. In fact, assume that $\tilde{u}_{ij} > \overline{u}$; then from (25) we have $u_{ij} = \overline{u}_{ij}$. Therefore $(v_{ij} - u_{ij}) \leqslant 0$ for any $v \in U_{adh}$. By inspection of (24) we see that $\hat{p}_{ij}(\tilde{u}_{ij}) < \hat{p}_{ij}(u_{ij})$. On the other hand we have

$$vu_{ij} - \hat{p}_{ij}(u_{ij}) < v\tilde{u}_{ij} - \hat{p}_{ij}(\tilde{u}_{ij}) = 0.$$

Similarly, if $\tilde{u}_{ij} < \underline{u}$ we take $u_{ij} = \underline{u}_{ij}$ and we have that $vu_{ij} - \hat{p}_{ij}(u_{ij}) > 0$ together with $(v_{ij} - u_{ij}) \geqslant 0$ for any $v \in U_{adh}$. Therefore $(vu - p) \cdot (v - u) \geqslant 0$ for all $v \in U_{adh}$. In case $v = 0$, it can be proved that the smoothing step defined above satisfies (7). Because of the 'projection' (25), the present iteration can be considered as belonging to the class of projected Gauss–Seidel schemes [9].

It should be clear that the formulation of the collective iterative scheme presented above applies also when $\tilde{\Delta}_h$ is used instead of Δ_h in one or both of the elliptic equations of our optimality system, replacing A_{ij} (resp. B_{ij}) with $\tilde{A}_{ij}$ (resp. $\tilde{B}_{ij}$) and c_{ij}^y (resp. c_{ij}^p) with $\tilde{c}_{ij}^y$ (resp. $\tilde{c}_{ij}^p$).

5. Multigrid schemes for nonlinear constrained optimal control problems

The multigrid algorithm presented here is based on the FAS [7] framework. This is a natural choice in the treatment of nonlinear problems, however, the present approach remains valid for the class of nonlinear multigrid (NMGM) methods discussed in [14]. Our choice is also motivated by the need of imposing constraints on the control variable which requires that this variable together with the state and the adjoint functions, and not their errors, be available at all levels. Another important aspect of the FAS scheme is that nonlinearities can be treated without the need of global linearization.

To illustrate the FAS method, consider first a generic nonlinear problem

$$A_h(u_h) = f_h, \tag{26}$$

where $A_h(\cdot)$ represents a nonlinear discrete operator on Ω_h.

Denote with $u_h^{(l)} = S_h\,(u_h^{(l-1)}, f_h)$ an appropriate smoothing scheme and suppose to apply m_1-times this iteration to (26) starting with the current approximation $u_h^{(0)}$ to obtain the approximate solution $\tilde{u}_h = u_h^{(m_1)}$. Now, the desired correction e_h to $\tilde{u}_h$ is defined by $A_h(\tilde{u}_h + e_h) = f_h$. This correction can be defined as the solution to

$$A_h(\tilde{u}_h + e_h) - A_h(\tilde{u}_h) = r_h, \tag{27}$$

where $r_h = f_h - A_h(\tilde{u}_h)$ is the residual associated to $\tilde{u}_h$.

Next, assume to represent problem (27) on the coarser grid Ω_H where $H = 2h$. To represent $\tilde{u}_h + e_h$ on the coarse grid we write

$$u_H := \dot{I}_h^H \tilde{u}_h + e_H. \tag{28}$$

Since $\dot{I}_h^H \tilde{u}_h$ and $\tilde{u}_h$ should represent the same function but on different grids, the standard choice of the fine-to-coarse restriction operator $\dot{I}_h^H$ is straight injection. We can think of representing e_h by a coarse function e_H because e_h is smooth due to the action of S_h.

Now to formulate (27) on the coarse grid replace $A_h(\cdot)$ by $A_H(\cdot)$, $\tilde{u}_h$ by $\dot{I}_h^H \tilde{u}_h$, and r_h by $I_h^H r_h = I_h^H(f_h - A_h(\tilde{u}_h))$. Here I_h^H is a conveniently chosen restriction operator. We get the following (FAS) equation:

$$A_H(u_H) = I_h^H(f_h - A_h(\tilde{u}_h)) + A_H(\dot{I}_h^H \tilde{u}_h). \tag{29}$$

This equation is also written in the form $A_H(u_H) = I_h^H f_h + \tau_h^H$ where

$$\tau_h^H = A_H(\dot{I}_h^H \tilde{u}_h) - I_h^H A_h(\tilde{u}_h).$$

The term τ_h^H is the fine-to-coarse defect or residual correction such that at convergence the solution to (29) coincides with the fine grid solution in the sense that $u_H = \dot{I}_h^H u_h$. With u_H obtained solving (29) and from (28) we have

$$e_H = u_H - \dot{I}_h^H \tilde{u}_h.$$

Therefore we can obtain a correction to the fine-grid approximation as follows $u_h = \tilde{u}_h + I_H^h e_H$ where I_H^h is a coarse-to-fine interpolation operator.

Therefore, we obtain the following FAS coarse-grid correction step:

$$u_h = \tilde{u}_h + I_H^h(u_H - \dot{I}_h^H \tilde{u}_h). \tag{30}$$

To damp possible high-frequency errors arising through the coarse-grid correction process, (30) is followed by m_2-times smoothing iteration.

A typical choice (in two dimensions) for I_H^h is bilinear interpolation and requiring that $(I_h^H u, v)_H = (u, I_H^h v)_h$ for all $u \in L_h^2$ and $v \in L_H^2$, a full-weighting restriction operator for I_h^H results. These operators are given in stencil form as follows

$$I_H^h = \frac{1}{4}\begin{bmatrix} 1 & 2 & 1 \\ 2 & 4 & 2 \\ 1 & 2 & 1 \end{bmatrix} \quad \text{and} \quad I_h^H = \frac{1}{16}\begin{bmatrix} 1 & 2 & 1 \\ 2 & 4 & 2 \\ 1 & 2 & 1 \end{bmatrix}. \tag{31}$$

In general, the solution of the coarse-grid problem (29) is obtained by defining a sequence of nested grids (also referred to as levels) $\Omega_k = \Omega_{h_k}$ of mesh size $h_k = h_1/2^{(k-1)}$, $k = 1, ..., L$, where $k = L$ is the finest level and h_1 is the mesh size of the coarsest grid. We can now denote all operators and functions in terms of the index k and define the multigrid FAS scheme as follows.

Multigrid FAS-(m_1, m_2) method for solving $A_k(u_k) = f_k$.

1. If $k = 1$ solve $A_k(u_k) = f_k$ directly (e.g., repeated application of S_k);
2. Pre-smoothing steps on the fine grid: $u_k^{(l)} = S_k(u_k^{(l-1)}, f_k)$, $l = 1, ..., m_1$;
3. Computation of the residual: $r_k = f_k - A_k u_k^{(m_1)}$;
4. Restriction of the residual: $r_{k-1} = I_k^{k-1} r_k$;
5. Set $u_{k-1} = \dot{I}_k^{k-1} u_k^{(m_1)}$;
6. Set $f_{k-1} = r_{k-1} + A_{k-1}(u_{k-1})$;
7. Call m times FAS-(m_1, m_2) to solve $A_{k-1}(u_{k-1}) = f_{k-1}$;
8. Coarse-grid correction: $u_k^{(m_1+1)} = u_k^{(m_1)} + I_{k-1}^k(u_{k-1} - \dot{I}_k^{k-1} u_k^{(m_1)})$;
9. Post-smoothing steps on the fine grid: $u_k^{(l)} = S_k(u_k^{(l-1)}, f_k)$, $l = m_1 + 2, ..., m_1 + m_2 + 1$;

Notice that we can perform m two-grid iterations at each working level. For $m = 1$ we have a V-cycle and for $m = 2$ we have a W-cycle; m is called the cycle index [29]. Our numerical experience shows that in case of constrained control problems the use of W-cycles results in a more robust multigrid iteration. In general, one application of the multigrid FAS-(m_1, m_2) scheme will not suffice. It must be repeatedly applied until a given tolerance is reached.

Now we specialize our description to problem (5) with the discretization scheme discussed above. We have the following system:

$$\Delta_k y_k + G(y_k) - u_k = f_k, \tag{32}$$

$$\Delta_k p_k + G'(y_k)\, p_k + y_k = z_k, \tag{33}$$

$$(\nu u_k - p_k) \cdot (v_k - u_k) \geqslant 0 \quad \text{for all } v_k \in U_{\text{ad}k}, \tag{34}$$

where $U_{\text{ad}k} = \{u \in L_k^2(\Omega_k) \mid \underline{u}(\mathbf{x}) \leqslant u(\mathbf{x}) \leqslant \overline{u}(\mathbf{x}) \text{ in } \Omega_k\}$.

Consider a current approximation to the solution of this system denoted by $\mathbf{w}_k = (y_k, p_k, u_k)$ and apply m_1-times the iterative scheme described in the previous section, so that the main components of the error that are left are smooth. Then we start a coarse-grid correction procedure to solve for these components. First, a coarse grid problem is constructed on the grid with mesh size h_{k-1} given by

$$\Delta_{k-1} y_{k-1} + G(y_{k-1}) - u_{k-1} = I_k^{k-1} f_k + \tau(y)_k^{k-1}, \tag{35}$$

$$\Delta_{k-1} p_{k-1} + G'(y_{k-1})\, p_{k-1} + y_{k-1} = I_k^{k-1} z_k + \tau(p)_k^{k-1}, \tag{36}$$

$$(\nu u_{k-1} - p_{k-1}) \cdot (v_{k-1} - u_{k-1}) \geqslant 0 \quad \text{for all} \quad v_{k-1} \in U_{\mathrm{ad}\,k-1},$$

where $\tau(y)_k^{k-1}$ and $\tau(p)_k^{k-1}$ are fine-to-coarse defect corrections defined by

$$\tau(y)_k^{k-1} = \Delta_{k-1} \dot{I}_k^{k-1} y_k + G(\dot{I}_k^{k-1} y_k) - \dot{I}_k^{k-1} u_k - I_k^{k-1}(\Delta_k y_k + G(y_k) - u_k), \tag{37}$$

$$\tau(p)_k^{k-1} = \Delta_{k-1} \dot{I}_k^{k-1} p_k + G'(\dot{I}_k^{k-1} y_k)\, \dot{I}_k^{k-1} p_k + \dot{I}_k^{k-1} y_k - I_k^{k-1}(\Delta_k p_k + G'(y_k)\, p_k + y_k). \tag{38}$$

Here $\dot{I}_k^{k-1}$ is straight injection and I_{k-1}^k, I_k^{k-1} are as in (31). Notice that the variational inequality defining the optimality condition has the same form on all grids.

Once the coarse grid problem is solved, which gives $\mathbf{w}_{k-1} = (y_{k-1}, p_{k-1}, u_{k-1})$, the coarse-grid correction follows:

$$y_k^{\mathrm{new}} = y_k + I_{k-1}^k (y_{k-1} - \dot{I}_k^{k-1} y_k), \tag{39}$$

$$p_k^{\mathrm{new}} = p_k + I_{k-1}^k (p_{k-1} - \dot{I}_k^{k-1} p_k), \tag{40}$$

$$u_k^{\mathrm{new}} = u_k + I_{k-1}^k (u_{k-1} - \dot{I}_k^{k-1} u_k). \tag{41}$$

This is followed by m_2 post-smoothing steps.

The application of N-times the FAS scheme is denoted by N-FAS. One can choose a starting working grid with a level number $K \leqslant L$ which is coarser than the finest grid where the solution is desired. In this case one applies N cycles of the FAS scheme on level K and then the solution is interpolated on the next finer grid. The interpolation provides a first approximation for the FAS iteration on this finer level and so on until the finest grid is reached. The combination of the nested iteration technique and the FAS scheme is called the full multigrid (FMG) method.

6. Local Fourier analysis

As mentioned in the previous section, the motivation for combining an iterative scheme with a coarse-grid correction is that these two schemes are effective on two complementary parts of the spectrum of the solution error. Therefore, we can think of characterizing the convergence properties of these two schemes and their combination by considering their representation on the Fourier space. This is indeed possible for linear or linearized problems without constraints. In these cases, a discrete operator in the physical space is represented by its Fourier symbol in the Fourier space, that is, its formal eigenvalue on the space of Fourier (eigen-)functions. This is advantageous to characterize important properties of the operator on the original physical space. For example, an iterative scheme whose symbol has an absolute value which is strictly smaller than one correspondingly to a part of the whole spectrum of Fourier modes is a converging iteration for those error components having frequencies of this part of spectrum.

We now proceed with a rigorous local Fourier analysis [8,29] to investigate the convergence properties of the two grid method applied to a linearized version of the optimality system (5) with no constraints on the control. This analysis represents an extension of previous work for second-order discretization [5] and can be extended to the three grid method following [30]. Results of numerical experiments presented in the following section show that the estimates given below may remain also valid in nonlinear constrained cases.

For the purpose of illustration, we consider the case where the Laplacian of the state equation is represented by the fourth-order accurate Δ_h and the Laplacian of the adjoint equation is the second-order $\tilde{\Delta}_h$. It is straightforward to repeat the discussion for the other configurations and estimates are given for all of them.

First, let us recall the local Fourier setting; see [29] for more details. Consider a sequence of (infinite) grids, $\Gamma_k = \{(ih_k, jh_k), i, j \in \mathbb{Z}\}$. On these grids we define the Fourier components:

$$\phi_k(\boldsymbol{\theta}, \mathbf{x}) = \mathrm{e}^{\mathrm{i}\theta_1 x_1/h_k}\, \mathrm{e}^{\mathrm{i}\theta_2 x_2/h_k}.$$

For any low frequency $\boldsymbol{\theta} = (\theta_1, \theta_2) \in [-\pi/2, \pi/2)^2$, we consider

$$\boldsymbol{\theta}^{(0,0)} := (\theta_1, \theta_2), \quad \boldsymbol{\theta}^{(1,1)} := (\overline{\theta_1}, \overline{\theta_2}),$$
$$\boldsymbol{\theta}^{(1,0)} := (\overline{\theta_1}, \theta_2), \quad \boldsymbol{\theta}^{(0,1)} := (\theta_1, \overline{\theta_2}),$$

where

$$\overline{\theta_i} = \begin{cases} \theta_i + \pi & \text{if } \theta_i < 0, \\ \theta_i - \pi & \text{if } \theta_i \geqslant 0. \end{cases}$$

We have $\phi(\boldsymbol{\theta}^{(0,0)}, \cdot) = \phi(\boldsymbol{\theta}^{(1,1)}, \cdot) = \phi(\boldsymbol{\theta}^{(1,0)}, \cdot) = \phi(\boldsymbol{\theta}^{(0,1)}, \cdot)$ for $\boldsymbol{\theta}^{(0,0)} \in [-\pi/2, \pi/2)^2$ and $(x_1, x_2) \in \Gamma_{k-1}$. That is, we have a quadruples of distinct Fourier components that coincide (aliases) on Γ_{k-1}.

Denote with $\boldsymbol{\alpha} = (\alpha_1, \alpha_2)$ and consider $\boldsymbol{\alpha} \in \{(0,0), (1,1), (1,0), (0,1)\}$; then on Γ_{k-1} we have $\phi_k(\boldsymbol{\theta}^{\boldsymbol{\alpha}}, \mathbf{x}) = \phi_{k-1}(2\boldsymbol{\theta}^{(0,0)}, \mathbf{x})$. The four components $\phi_k(\boldsymbol{\theta}^{\boldsymbol{\alpha}}, \cdot)$ are called harmonics. Their span is denoted with

$$E_k^{\theta} = \mathrm{span}[\phi_k(\boldsymbol{\theta}^{\boldsymbol{\alpha}}, \cdot) : \boldsymbol{\alpha} \in \{(0,0), (1,1), (1,0), (0,1)\}].$$

Purpose of this analysis is to investigate the action of the smoothing and coarse-grid correction operators on couples (e_y, e_p) defined by

$$e_y(\mathbf{x}) = \sum_{\boldsymbol{\alpha}, \boldsymbol{\theta}} Y_{\boldsymbol{\alpha}, \boldsymbol{\theta}}\, \phi_k(\boldsymbol{\theta}^{\boldsymbol{\alpha}}, \mathbf{x}) \quad \text{and} \quad e_p(\mathbf{x}) = \sum_{\boldsymbol{\alpha}, \boldsymbol{\theta}} P_{\boldsymbol{\alpha}, \boldsymbol{\theta}}\, \phi_k(\boldsymbol{\theta}^{\boldsymbol{\alpha}}, \mathbf{x}).$$

Here (e_y, e_p) represent the error functions for y_h and p_h and $W_{\boldsymbol{\alpha}, \boldsymbol{\theta}} = (Y_{\boldsymbol{\alpha}, \boldsymbol{\theta}}, P_{\boldsymbol{\alpha}, \boldsymbol{\theta}})$ denote the corresponding Fourier coefficients. With this decomposition of the error, the action of one smoothing step can be expressed as $W^{(1)}_{\boldsymbol{\alpha}, \boldsymbol{\theta}} = \hat{S}(\boldsymbol{\alpha}, \boldsymbol{\theta})\, W^{(0)}_{\boldsymbol{\alpha}, \boldsymbol{\theta}}$ where $\hat{S}(\boldsymbol{\alpha}, \boldsymbol{\theta})$ is the Fourier symbol [29] of the smoothing operator. To determine $\hat{S}(\boldsymbol{\alpha}, \boldsymbol{\theta})$, recall that the functions $\phi_k(\boldsymbol{\theta}^{\boldsymbol{\alpha}}, \mathbf{x})$ are eigenfunctions of any discrete operator described by a difference stencil on the Γ_k grid. Therefore, we have $S_k \phi_k(\boldsymbol{\theta}^{\boldsymbol{\alpha}}, \mathbf{x}) = \hat{S}_k(\boldsymbol{\alpha}, \boldsymbol{\theta})\, \phi_k(\boldsymbol{\theta}, \mathbf{x})$ that is, the symbol of S_k is its (formal) eigenvalue.

Now, consider one collective Gauss–Seidel iteration step applied to the following problem:

$$\Delta_h y_h + g\, y_h - p_h/v = f_h, \tag{42}$$
$$\tilde{\Delta}_h p_h + g\, p_h + y_h = z_h. \tag{43}$$

In this case, one smoothing step at $\mathbf{x}$ corresponds to an update which sets the residuals at $\mathbf{x}$ equal to zero. In terms of Fourier modes $\boldsymbol{\theta}$, $\hat{S}_k(\boldsymbol{\theta})$ is given by

$$\begin{bmatrix} \frac{1}{12}[-(\mathrm{e}^{-2\mathrm{i}\theta_1} + \mathrm{e}^{-2\mathrm{i}\theta_2}) + 16\,(\mathrm{e}^{-\mathrm{i}\theta_1} + \mathrm{e}^{-\mathrm{i}\theta_2}) - 60] + h^2 g & -h_k^2/v \\ h_k^2 & (\mathrm{e}^{-\mathrm{i}\theta_1} + e^{-\mathrm{i}\theta_2} - 4) + h_k^2\, g \end{bmatrix}^{-1}$$
$$\times \begin{bmatrix} -\frac{1}{12}[-(\mathrm{e}^{-2\mathrm{i}\theta_1} + \mathrm{e}^{-2\mathrm{i}\theta_2}) + 16\,(\mathrm{e}^{-\mathrm{i}\theta_1} + \mathrm{e}^{-\mathrm{i}\theta_2})] & 0 \\ 0 & -(\mathrm{e}^{\mathrm{i}\theta_1} + \mathrm{e}^{\mathrm{i}\theta_2}) \end{bmatrix}.$$

The smoothing property of S_k measures the action of this iteration on the high-frequency error components and can be defined as follows:

$$\mu(S_k) = \sup\{r(\hat{S}_k(\boldsymbol{\theta})) :\ \boldsymbol{\theta} \in \{\boldsymbol{\theta}^{(1,1)}, \boldsymbol{\theta}^{(1,0)}, \boldsymbol{\theta}^{(0,1)}\}\}, \tag{44}$$

where r denotes the spectral radius and $\mu(\cdot)$ is the smoothing factor which can be evaluated for any choice of values of h and v.

The next step is to construct the Fourier symbol of the twogrid coarse-grid correction operator

$$CG_k^{k-1} = [I_k - I_{k-1}^k\, (A_{k-1})^{-1}\, I_k^{k-1}\, A_k].$$

We denote the corresponding symbol by

$$\widehat{CG}_k^{k-1}(\boldsymbol{\theta}) = [\hat{I}_k - \hat{I}_{k-1}^k(\boldsymbol{\theta})\,(\widehat{A}_{k-1}(2\boldsymbol{\theta}))^{-1}\,\hat{I}_k^{k-1}(\boldsymbol{\theta})\,\widehat{A}_k(\boldsymbol{\theta})].$$

The symbol of the coarse grid operator $\widehat{A}_{k-1}(\boldsymbol{\theta})$ is

$$\begin{bmatrix} \dfrac{1}{6h_{k-1}^2}[-(\cos(4\theta_1)+\cos(4\theta_2))+16\,(\cos(2\theta_1)+\cos(2\theta_2))-30]+g & -1/v \\ 1 & \dfrac{2(\cos(2\theta_1)+\cos(2\theta_2))-4}{h_{k-1}^2}+g \end{bmatrix},$$

(notice the different symbols for the different discretization of the Laplacian) and similarly one constructs $\widehat{A}_k(\boldsymbol{\theta})$ corresponding to the four harmonics, that is,

$$\begin{bmatrix} l(\boldsymbol{\theta}^{(0,0)}) & 0 & 0 & 0 & -1/v & 0 & 0 & 0 \\ 0 & l(\boldsymbol{\theta}^{(1,1)}) & 0 & 0 & 0 & -1/v & 0 & 0 \\ 0 & 0 & l(\boldsymbol{\theta}^{(1,0)}) & 0 & 0 & 0 & -1/v & 0 \\ 0 & 0 & 0 & l(\boldsymbol{\theta}^{(0,1)}) & 0 & 0 & 0 & -1/v \\ 1 & 0 & 0 & 0 & \tilde{l}(\boldsymbol{\theta}^{(0,0)}) & 0 & 0 & 0 \\ 0 & 1 & 0 & 0 & 0 & \tilde{l}(\boldsymbol{\theta}^{(1,1)}) & 0 & 0 \\ 0 & 0 & 1 & 0 & 0 & 0 & \tilde{l}(\boldsymbol{\theta}^{(1,0)}) & 0 \\ 0 & 0 & 0 & 1 & 0 & 0 & 0 & \tilde{l}(\boldsymbol{\theta}^{(0,1)}) \end{bmatrix},$$

where

$$l(\boldsymbol{\theta}^{\boldsymbol{\alpha}}) = \frac{1}{6h_k^2}[-(\cos(2\theta_1^{\alpha_1}) + \cos(2\theta_2^{\alpha_2})) + 16\,(\cos(\theta_1^{\alpha_1}) + \cos(\theta_2^{\alpha_2})) - 30] + g$$

and

$$\tilde{l}(\boldsymbol{\theta}^{\boldsymbol{\alpha}}) = \frac{2(\cos(\theta_1^{\alpha_1}) + \cos(\theta_2^{\alpha_2})) - 4}{h_k^2}.$$

The symbol of restriction operator is

$$\hat{I}_k^{k-1}(\boldsymbol{\theta}) = \begin{bmatrix} I(\boldsymbol{\theta}^{(0,0)}) & I(\boldsymbol{\theta}^{(1,1)}) & I(\boldsymbol{\theta}^{(1,0)}) & I(\boldsymbol{\theta}^{(0,1)}) & 0 & 0 & 0 & 0 \\ 0 & 0 & 0 & 0 & I(\boldsymbol{\theta}^{(0,0)}) & I(\boldsymbol{\theta}^{(1,1)}) & I(\boldsymbol{\theta}^{(1,0)}) & I(\boldsymbol{\theta}^{(0,1)}) \end{bmatrix},$$

where

$$I(\boldsymbol{\theta}^{\boldsymbol{\alpha}}) = \tfrac{1}{4}(1 + \cos(\theta_1^{\alpha_1}))(1 + \cos(\theta_2^{\alpha_2})).$$

For the prolongation operator we have $\hat{I}_{k-1}^k(\boldsymbol{\theta}) = \hat{I}_k^{k-1}(\boldsymbol{\theta})^{\mathrm{T}}$.

Finally, the symbol of the two grid method is given by

$$\widehat{TG}_k^{k-1}(\boldsymbol{\theta}) = \hat{S}_k(\boldsymbol{\theta})^{m_2}\,\widehat{CG}_k^{k-1}(\boldsymbol{\theta})\,\hat{S}_k(\boldsymbol{\theta})^{m_1}.$$

This is an 8×8 matrix corresponding to the four pairs $(Y_{\boldsymbol{\alpha},\boldsymbol{\theta}}, P_{\boldsymbol{\alpha},\boldsymbol{\theta}})$, $\boldsymbol{\alpha} \in \{(0,0), (1,1), (1,0), (0,1)\}$. In this framework the convergence factor is defined as follows:

$$\eta(TG_k^{k-1}) = \sup\{r(\widehat{TG}_k^{k-1}(\boldsymbol{\theta})) : \boldsymbol{\theta} \in [-\pi/2, \pi/2)^2\}.$$

We can state the following theorem.

Table 1
Convergence factors and smoothing factors; $h = \frac{1}{64}$, $g = 20$

$\Delta_h y$, $\Delta_h p$		Local Fourier analysis	
(m_1, m_2)	ν	$\mu(S_k)$	$\eta(TG_k^{k-1})$
(1,1)	10^{-4}	0.5362	0.2429
(2,2)	10^{-4}	0.5362	0.1233
(1,1)	10^{-8}	0.6089	0.3457
(2,2)	10^{-8}	0.6089	0.1933
$\Delta_h y$, $\tilde{\Delta}_h p$		Local Fourier analysis	
(1,1)	10^{-4}	0.5346	0.2413
(2,2)	10^{-4}	0.5346	0.1215
(1,1)	10^{-8}	0.5787	0.3094
(2,2)	10^{-8}	0.5787	0.1566
$\tilde{\Delta}_h y$, $\Delta_h p$		Local Fourier analysis	
(1,1)	10^{-4}	0.5346	0.2413
(2,2)	10^{-4}	0.5346	0.1215
(1,1)	10^{-8}	0.5787	0.3094
(2,2)	10^{-8}	0.5787	0.1566
$\tilde{\Delta}_h y$, $\tilde{\Delta}_h p$		Local Fourier analysis	
(1,1)	10^{-4}	0.5020	0.1939
(2,2)	10^{-4}	0.5020	0.0851
(1,1)	10^{-8}	0.5491	0.2772
(2,2)	10^{-8}	0.5491	0.1255

Theorem 2. *Under the assumption that all multigrid components are linear and that* $(\mathscr{A}_{k-1})^{-1}$ *exists and* $\hat{\mathscr{S}}_k(\boldsymbol{\theta})$: $E_k^\theta \times E_k^\theta \to E_k^\theta \times E_k^\theta$ *for all* $\boldsymbol{\theta} \in [-\pi/2, \pi/2)^2$, *we have a representation of the twogrid operator* TG_k^{k-1} *on* $E_k^\theta \times E_k^\theta$ *by a* 8×8 *matrix given by*

$$\widehat{TG}_k^{k-1}(\boldsymbol{\theta}) = \hat{\mathscr{S}}_k(\boldsymbol{\theta})^{m_2}\, \widehat{CG}_k^{k-1}(\boldsymbol{\theta})\, \hat{\mathscr{S}}_k(\boldsymbol{\theta})^{m_1},$$

and for given mesh with mesh-size h_k *and given weight of the cost* ν, *the convergence factor estimate for the twogrid scheme applied to* (42)–(43) *is given by*

$$\eta(TG_k^{k-1}) = \sup\{r(\widehat{TG}_k^{k-1}(\boldsymbol{\theta})) : \boldsymbol{\theta} \in [-\pi/2, \pi/2)^2\}.$$

In Table 1, values of $\mu(S_k)$ and of $\eta(TG_k^{k-1})$ corresponding to the setting $h_k = \frac{1}{64}$ and $\nu \in \{10^{-4}, 10^{-8}\}$ and $g = 20$ are reported. These values are reported for all possible configuration of discretization schemes and are found to be similar. Almost identical values are obtained for $g \in [-200, 200]$. The values of μ and η are slightly worse for coarse $h_k \in [\frac{1}{16}, \frac{1}{4}]$ and remain close to the values given in Table 1 for finer meshes. In all cases, it is verified that $(\mathscr{A}_{k-1})$ is not singular as required in Theorem 2.

These results show robustness of the multigrid solver with respect to values of ν and suggest mesh independence. The values reported for $\mu(S_k)$ are quite close to the value of the smoothing factor of the Gauss–Seidel scheme applied to the Poisson problem, suggesting that the iteration constructed in Section 4 is a good smoother. The convergence factors estimates reported in Table 1 predict typical multigrid convergence behavior of the proposed multigrid scheme applied to linear unconstrained problems.

7. Numerical experiments

We present a numerical investigation of the approximation properties of the finite-difference schemes discussed above and of the computational performance of the proposed multigrid method to solve constrained optimal control problems. Results of three series of experiments are reported. For all cases we choose $G(y) = y^4$ and $\Omega = (0, 1) \times (0, 1)$.

First, we remark that in unconstrained cases using fourth-order schemes with typical smooth test functions, $\mathcal{O}(h^4)$ accuracy is obtained. Further, we can show that second-order accuracy is obtained whenever the second-order discrete Laplacian is used to approximate the state and/or the adjoint equations.

Next, the question arises of how the fourth-order discretization performs in less regular cases. For this purpose, we consider the case of unconstrained control with a setting such that the continuous solution is less regular than the degree required from Theorem 1. In the second series of experiments, we choose a problem with constrained control with $v > 0$. In this experiment and the previous one, we find that higher-order approximation of the state equation is more advantageous than higher-order approximation of the adjoint equation in the sense that more accurate solutions are obtained. This in turn demonstrates a tight relationship between accuracies of approximation of the state and control functions.

In the last series of experiments we consider a bang-bang control situation which demonstrates that our multigrid scheme can be advantageously used to investigate the setting $v = 0$ with constraints on the control.

Results of experiments are reported concerning the tracking functional $|y_h - \tilde{R}_h z|_0$ depending on the value of the cost of the control v. We also report values of the observed convergence factor defined as the "asymptotic" value of the ratio between the discrete L^2-norm of the residuals resulting from two successive multigrid cycles on a given mesh [14]. For the coarsest grid we have $h_1 = \frac{1}{8}$ and we use up to nine levels. We use $m_1 = m_2 = 2$ smoothing steps and the FMG version of the FAS algorithm with initial level $K = 3$. For all experiments, the starting guess is the zero function. In the FMG process we apply three FAS cycles for working levels less than L. The stopping criterion is $|r_h(y)|_0 + |r_h(p)|_0 < 10^{-10}$ which is usually attained before 10 cycles at the finest grid.

7.1. Case I: an unconstrained optimal control problem

We discuss an unconstrained control problem with a state $y \notin C^6(\bar{\Omega})$ whose regularity is less than that required for Theorem 1 to have fourth-order accuracy. This function was proposed by Schaffer in [26] to test convergence behavior of fourth-order schemes. Schaffer's function is defined as follows. Take $T(x_1, x_2) = x_2 - x_1^2 + x_1 - \frac{3}{4}$ and define the following discontinuous function

$$C(x_1, x_2) = \begin{cases} 1, & T(x_1, x_2) > 0, \\ -1, & T(x_1, x_2) \leqslant 0. \end{cases}$$

As exact solution for the state equation we choose $y(x_1, x_2) = \exp(C(x_1, x_2)\, T(x_1, x_2)^6)$. Notice that $y \notin C^6(\bar{\Omega})$ because it has a jump discontinuity in the 6th derivatives along the parabola $T(x_1, x_2) = 0$. Further we take $f = \Delta y$ and $u = G(y)$. Correspondingly, the exact adjoint variable solution is given by $p = v\, G(y)$ and as target function we have $z = y + \Delta p + G'(y)\, p$. For this experiment we use the V-cycle setting.

Results for this case are reported in Table 2. First, notice that the measured convergence factors for this case resemble those of multigrid for Poisson's problem and lie slightly below those predicted by the local Fourier analysis of Section 6. Also notice that CPU times scale linearly with $1/h^2$. So for this case see mesh independent convergence. We also remark that the CPU time for the fourth-order scheme is approximately 30% more than that required by the second-order scheme while providing four orders of magnitude better accuracy. Further notice that as v is decreased more favorable tracking errors are obtained. Concerning accuracy errors, we do not always obtain fourth-order convergence by refinement, especially when h is sufficiently small. On the other hand, when second-order approximation of the Laplacian is used we see $\mathcal{O}(h^2)$ convergence. The use of the higher-order scheme is advantageous as far as this scheme is used to represent the state equation, since much better accuracy of the optimal solutions is obtained in this case. However, the results reported in Table 2 show that the requirements on the regularity of the optimal solution stated in Theorem 1 are necessary to guarantee higher-order accuracy.

7.2. Case II: a constrained optimal control problem

Now, a constrained optimal control problem is considered. The exact solution for this case is constructed as follows. Define

$$\begin{aligned} f &= -u + \Delta y + G(y), \\ z &= y + \Delta p + G'(y)\, p, \end{aligned} \tag{45}$$

Table 2
Convergence results for Case I

ν	mesh	$\|y_h - R_h y\|_0$	$\|p_h - R_h p\|_0$	$\|u_h - R_h u\|_0$	$\|y_h - \tilde{R}_h z\|_0$	η	CPU s
$\Delta_h y, \Delta_h p$							
10^{-4}	128×128	0.39(−9)	0.49(−11)	0.49(−7)	0.57(−3)	0.086	0.25
10^{-4}	256×256	0.27(−10)	0.31(−12)	0.31(−8)	0.57(−3)	0.085	0.87
10^{-4}	512×512	0.18(−11)	0.21(−13)	0.21(−9)	0.58(−3)	0.085	2.98
10^{-4}	1024×1024	0.17(−12)	0.11(−14)	0.11(−10)	0.58(−3)	0.082	10.81
10^{-8}	128×128	0.28(−10)	0.25(−14)	0.25(−6)	0.57(−7)	0.075	0.15
10^{-8}	256×256	0.65(−12)	0.15(−15)	0.15(−7)	0.57(−7)	0.080	0.82
10^{-8}	512×512	0.32(−13)	0.11(−16)	0.11(−8)	0.58(−7)	0.085	2.92
10^{-8}	1024×1024	0.86(−14)	0.16(−17)	0.16(−9)	0.58(−7)	0.085	10.84
$\Delta_h y, \tilde{\Delta}_h p$							
10^{-4}	128×128	0.48(−7)	0.33(−9)	0.33(−5)	0.57(−3)	0.086	0.15
10^{-4}	256×256	0.12(−7)	0.84(−10)	0.84(−6)	0.57(−3)	0.085	0.78
10^{-4}	512×512	0.30(−8)	0.21(−10)	0.21(−6)	0.58(−3)	0.086	2.87
10^{-4}	1024×1024	0.75(−9)	0.53(−11)	0.53(−7)	0.58(−3)	0.082	9.84
10^{-8}	128×128	0.31(−10)	0.26(−14)	0.26(−6)	0.57(−7)	0.070	0.20
10^{-8}	256×256	0.40(−11)	0.14(−15)	0.14(−7)	0.57(−7)	0.090	0.75
10^{-8}	512×512	0.97(−12)	0.21(−16)	0.21(−8)	0.58(−7)	0.090	2.87
10^{-8}	1024×1024	0.24(−12)	0.63(−17)	0.63(−9)	0.58(−7)	0.085	9.87
$\tilde{\Delta}_h y, \Delta_h p$							
10^{-4}	128×128	0.14(−5)	0.16(−7)	0.16(−3)	0.57(−3)	0.046	0.12
10^{-4}	256×256	0.35(−6)	0.42(−8)	0.42(−4)	0.57(−3)	0.043	0.64
10^{-4}	512×512	0.88(−7)	0.10(−8)	0.10(−4)	0.58(−3)	0.042	2.34
10^{-4}	1024×1024	0.22(−7)	0.26(−9)	0.26(−5)	0.58(−3)	0.042	9.43
10^{-8}	128×128	0.61(−8)	0.42(−11)	0.42(−3)	0.54(−7)	0.060	0.18
10^{-8}	256×256	0.15(−8)	0.10(−11)	0.10(−3)	0.57(−7)	0.060	0.68
10^{-8}	512×512	0.39(−9)	0.26(−12)	0.26(−4)	0.58(−7)	0.050	2.28
10^{-8}	1024×1024	0.99(−10)	0.66(−13)	0.66(−5)	0.58(−7)	0.046	7.84
$\tilde{\Delta}_h y, \tilde{\Delta}_h p$							
10^{-4}	128×128	0.13(−5)	0.17(−7)	0.17(−3)	0.57(−3)	0.040	0.15
10^{-4}	256×256	0.34(−6)	0.43(−8)	0.43(−4)	0.57(−3)	0.041	0.48
10^{-4}	512×512	0.86(−7)	0.10(−8)	0.10(−4)	0.58(−3)	0.040	2.10
10^{-4}	1024×1024	0.21(−7)	0.26(−9)	0.26(−5)	0.58(−3)	0.040	7.56
10^{-8}	128×128	0.61(−8)	0.42(−11)	0.42(−3)	0.54(−7)	0.036	0.10
10^{-8}	256×256	0.15(−8)	0.10(−11)	0.10(−3)	0.57(−7)	0.040	0.45
10^{-8}	512×512	0.39(−9)	0.26(−12)	0.26(−4)	0.58(−7)	0.040	2.10
10^{-8}	1024×1024	0.99(−10)	0.66(−13)	0.66(−5)	0.58(−7)	0.040	7.10

where

$$y(x_1, x_2) = \sin(2\pi x_1)\sin(2\pi x_2),$$
$$p(x_1, x_2) = \nu\ \sin(2\pi x_1)\sin(2\pi x_2),$$
$$u(x_1, x_2) = \max\{-1/2,\ \min\{1/2,\ p(x_1, x_2)/\nu\}\}.$$

With this setting the control is active as it can be seen in Fig. 1. We use W-cycles.

Results of numerical experiments with Case II are reported in Table 3 for every second grid refinement. In this case the exact state and adjoint optimal solutions possess the degree of smoothness required in Theorem 1 in order to have fourth-order accuracy assuming no constraints. On the other hand, because of active constraints the control can be only H^1. The numerical results reported in Table 3 (top) demonstrate that using fourth-order schemes for the state and adjoint

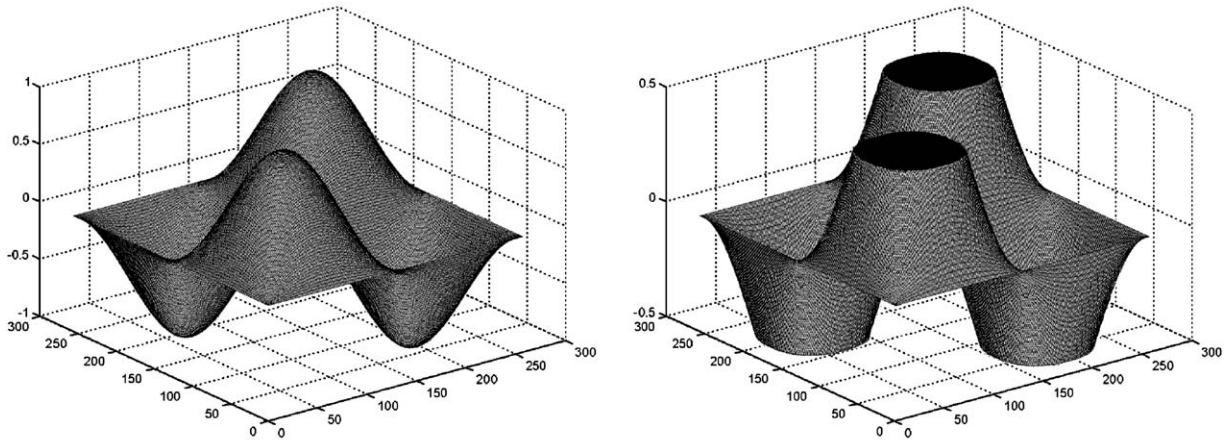

Fig. 1. Numerical solution for Case II, $\nu = 10^{-6}$. The state (left) and the control (right); 256×256 mesh.

Table 3
Convergence results for Case II

ν	mesh	$\lvert y_h - R_h y\rvert_0$	$\lvert p_h - R_h p\rvert_0$	$\lvert u_h - R_h u\rvert_0$	$\lvert y_h - \tilde{R}_h z\rvert_0$	η	CPU s
$\Delta_h y, \Delta_h p$							
10^{-3}	64×64	0.49(−6)	0.68(−8)	0.28(−5)	0.39(−1)	0.113	0.14
10^{-3}	256×256	0.19(−8)	0.27(−10)	0.11(−7)	0.39(−1)	0.100	1.23
10^{-3}	1024×1024	0.76(−11)	0.10(−12)	0.43(−10)	0.39(−1)	0.115	13.59
10^{-6}	64×64	0.14(−6)	0.80(−9)	0.99(−4)	0.39(−4)	0.262	0.28
10^{-6}	256×256	0.55(−9)	0.31(−11)	0.39(−6)	0.39(−4)	0.116	1.28
10^{-6}	1024×1024	0.21(−11)	0.12(−13)	0.15(−8)	0.39(−4)	0.117	13.50
$\Delta_h y, \tilde{\Delta}_h p$							
10^{-3}	64×64	0.49(−6)	0.39(−6)	0.16(−3)	0.39(−1)	0.112	0.10
10^{-3}	256×256	0.54(−7)	0.24(−7)	0.99(−5)	0.39(−1)	0.115	1.26
10^{-3}	1024×1024	0.35(−8)	0.15(−8)	0.62(−6)	0.39(−1)	0.114	12.68
10^{-6}	64×64	0.14(−6)	0.86(−9)	0.10(−3)	0.39(−4)	0.275	0.12
10^{-6}	256×256	0.18(−8)	0.62(−11)	0.77(−6)	0.39(−4)	0.116	1.26
10^{-6}	1024×1024	0.11(−9)	0.20(−12)	0.25(−7)	0.39(−4)	0.117	12.81
$\tilde{\Delta}_h y, \Delta_h p$							
10^{-3}	64×64	0.39(−3)	0.50(−5)	0.20(−2)	0.39(−1)	0.04	0.05
10^{-3}	256×256	0.24(−4)	0.31(−6)	0.12(−3)	0.39(−1)	0.04	0.82
10^{-3}	1024×1024	0.15(−5)	0.19(−7)	0.80(−5)	0.39(−1)	0.03	12.34
10^{-6}	64×64	0.14(−3)	0.10(−5)	0.78(−1)	0.16(−3)	0.130	0.17
10^{-6}	256×256	0.71(−5)	0.40(−7)	0.48(−2)	0.42(−4)	0.03	1.00
10^{-6}	1024×1024	0.43(−6)	0.24(−8)	0.30(−3)	0.39(−4)	0.04	15.82
$\tilde{\Delta}_h y, \tilde{\Delta}_h p$							
10^{-3}	64×64	0.39(−3)	0.54(−5)	0.22(−2)	0.39(−1)	0.04	0.07
10^{-3}	256×256	0.24(−4)	0.33(−6)	0.13(−3)	0.39(−1)	0.04	0.81
10^{-3}	1024×1024	0.15(−5)	0.21(−7)	0.86(−5)	0.39(−1)	0.03	10.79
10^{-6}	64×64	0.14(−3)	0.10(−5)	0.78(−1)	0.16(−3)	0.120	0.03
10^{-6}	256×256	0.71(−5)	0.40(−7)	0.48(−2)	0.42(−4)	0.03	0.82
10^{-6}	1024×1024	0.43(−6)	0.24(−8)	0.30(−3)	0.39(−4)	0.04	13.29

Table 4
Convergence results for Case III

V-cycle	$\Delta_h y\ \Delta_h p$		$\tilde{\Delta}_h y,\ \tilde{\Delta}_h p$	
mesh	η	CPU s	η	CPU s
128×128	0.45	0.35	0.40	0.25
256×256	0.45	1.39	0.52	1.01
512×512	0.45	5.10	0.50	3.95
1024×1024	0.45	21.29	0.45	15.98
2048×2048	0.45	87.28	0.45	64.07
W-cycle				
128×128	0.12	0.60	0.23	0.37
256×256	0.19	2.09	0.27	1.48
512×512	0.31	7.85	0.28	6.09
1024×1024	0.39	31.45	0.25	24.87
2048×2048	0.30	131.85	0.30	97.25

equations, fourth-order convergent optimal solutions can be obtained also in the presence of active constraints. In fact, the values of the norms $|y_h - R_h y|_0$, $|p_h - R_h p|_0$, and in particular of $|u_h - R_h u|_0$ scale as a factor of approximately 16^2 every second mesh refinement. This is a surprising result, especially regarding the control function, considering the known accuracy estimates for control-constrained problems [4,17,22,25] and the limitation in the regularity of the control function due to the presence of constraints.

In the other configurations, where the second-order scheme is used to approximate the state and/or the adjoint equations, second-order convergence of solutions (including the control) is obtained. That is, the values of the norms $|y_h - R_h y|_0$, $|p_h - R_h p|_0$, and $|u_h - R_h u|_0$ scale as a factor of approximately 16 every second mesh refinement. In this case we observe that higher-order approximation of the state equation is more advantageous than better approximation of the adjoint operator. In fact, while the order of convergence is the same, the magnitude of values of the error norms is much larger with the $(\tilde{\Delta}_h y, \Delta_h p)$ scheme than with the $(\Delta_h y, \tilde{\Delta}_h p)$ scheme.

Regarding convergence of the multigrid scheme for the present constrained case, convergence factors close to those predicted by Fourier analysis are obtained; see Table 3.

7.3. Case III: bang-bang control

We complete this numerical investigation by presenting results of computation for the case $\nu = 0$ and box constraints $\underline{u} = -1$ and $\overline{u} = 1$. We consider the nonlinear setting above with homogeneous Dirichlet boundary conditions and a target function given by

$$z(x_1, x_2) = \sin(4\pi x_1).$$

Notice that this function is not everywhere zero on the boundary of Ω and therefore it is not attainable by any control. With this choice, a bang-bang type control solution is obtained. The purpose of this experiment is to demonstrate the ability of the multigrid algorithm to solve bang-bang optimal control problems. We also consider Case III to compare the V- and W-cycles which appear to have different behavior (Table 4). In this case, the tracking ability is limited by the presence of constraints and for all experiments reported below we have $|y_h - \tilde{R}_h z|_0 \approx 0.70$. A numerical solution for Case III is depicted in Fig. 2. Clearly, this is a limit case for our algorithm and the resulting convergence factors worsen. Nevertheless, especially for the V-cycle we notice mesh independency. The W-cycle provides better convergence rates as the V-cycle even if an unpredictable dependence on the mesh-size can be observed. However, notice that the V-cycle has a favorable computational cost with respect to the W-cycle.

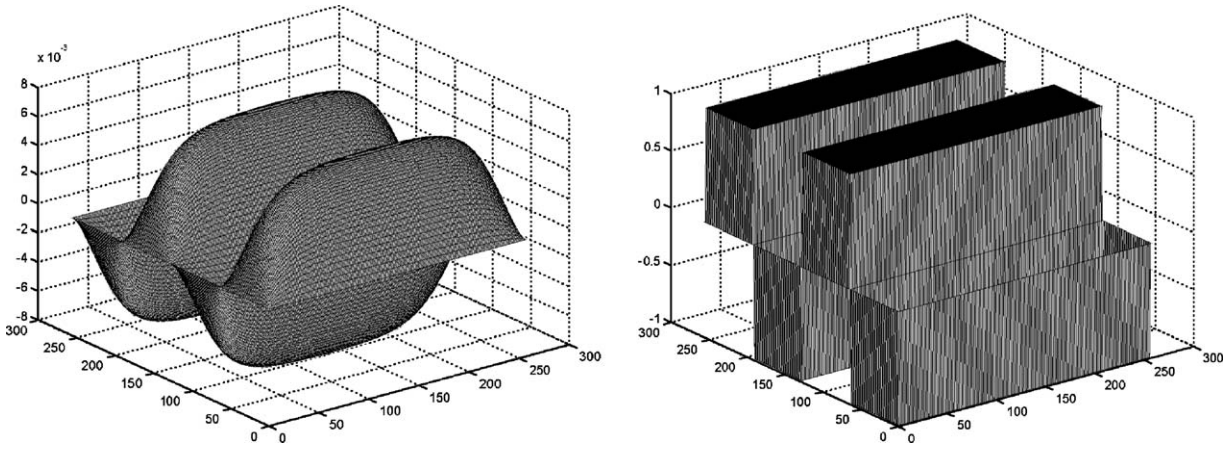

Fig. 2. Numerical solution for the bang–bang problem. The state (left) and the control (right); 256 × 256 mesh.

8. Conclusions

Accuracy estimates and convergence behavior for higher- and mixed-order finite-difference discretization of optimality systems were discussed. For the solution of these systems, an efficient and robust multigrid algorithm for nonlinear constrained optimal control problems was presented. Results of numerical experiments showed that fourth-order accurate optimal solutions, including the control function, can be obtained also when constraints are active. In general, we found that higher-order approximation of the state equation is more advantageous than better approximation of the adjoint operator. Further results demonstrated the ability of the multigrid scheme in solving constrained optimal control problems also in the limit case of bang-bang control.

References

[1] N. Arada, E. Casas, F. Tröltzsch, Error estimates for a semilinear elliptic control problem, Comput. Optim. Appl. 23 (2002) 201–229.
[2] E. Arian, S. Ta'asan, Smoothers for optimization problems, in: N. Duane Melson, T.A. Manteuffel, S.F. McCormick, C.C. Douglas, (Eds.), Seventh Copper Mountain Conference on Multigrid Methods, vol. CP3339, NASA Conference Publication, NASA, Hampton, VA, 1995, pp. 15–30.
[3] A. Borzì, K. Kunisch, The numerical solution of the steady state solid fuel ignition model and its optimal control, SIAM J. Sci. Comput. 22 (1) (2000) 263–284.
[4] A. Borzì, K. Kunisch, A multigrid scheme for elliptic constrained optimal control problems, Comput. Optim. Appl. 31 (2005) 309–333.
[5] A. Borzì, K. Kunisch, D.Y. Kwak, Accuracy and convergence properties of the finite difference multigrid solution of an optimal control optimality system, SIAM J. Control Opt. 41 (2003) 1477–1497.
[6] J.H. Bramble, B.E. Hubbard, On a finite difference analogue of an elliptic boundary problem which is neither diagonally dominant nor of non-negative type, J. Math. Phys. 43 (1964) 117–132.
[7] A. Brandt, Multi-level adaptive solutions to boundary-value problems, Math. Comput. 31 (1977) 333–390.
[8] A. Brandt, Rigorous quantitative analysis of multigrid, I: constant coefficients two-level cycle with L_2-norm, SIAM J. Numer. Anal. 31 (1994) 1695–1730.
[9] A. Brandt, C.W. Cryer, Multi-grid algorithms for the solution of linear complementarity problems arising from free boundary problems, SIAM J. Sci. Statist. Comput. 4 (1983) 655–684.
[10] Th. Dreyer, B. Maar, V. Schulz, Multigrid optimization in applications, J. Comput. Appl. Math. 120 (2000) 67–84.
[11] K. Glashoff, E. Sachs, On theoretical and numerical aspects of the bang-bang principle, Numer. Math. 29 (1977) 93–113.
[12] H. Goldberg, F. Tröltzsch, Second order sufficient optimality conditions for a class of non-linear parabolic boundary control problems, SIAM J. Control Optim. 31 (1993) 1007–1027.
[13] W. Hackbusch, Fast solution of elliptic control problems, J. Optim. Theory Appl. 31 (1980) 565–581.
[14] W. Hackbusch, Multi-grid Methods and Applications, Springer, New York, 1985.
[15] W. Hackbusch, Elliptic Differential Equations, Springer, New York, 1992.
[16] M. Hintermüller, M. Ulbrich, A mesh-independence result for semismooth Newton methods, Math. Programming 101 (2004) 151–184.
[17] M. Hinze, A variational discretization concept in control constrained optimization: the linear-quadratic case, Comput. Optim. Appl. 30 (2005) 45–63.
[18] A. Kauffmann, Optimal control of the solid fuel ignition model, Ph.D. Thesis, Technical University of Berlin, Berlin, 1998.
[19] J.L. Lions, Optimal Control of Systems Governed by Partial Differential Equations, Springer, Berlin, 1971.

[20] J.L. Lions, Control of Distributed Singular Systems, Gauthier-Villars, Paris, 1985.
[21] K. Malanowski, Convergence of approximations vs. regularity of solutions for convex, control-constrained optimal-control problems, Appl. Math. Optim. 8 (1981) 69–95.
[22] C. Meyer, A. Rösch, Superconvergence properties of optimal control problems, SIAM J. Control Optim. 43 (2004) 970–985.
[23] C.V. Pao, Nonlinear Parabolic and Elliptic Equations, Plenum Press, New York, 1992.
[24] L. Qi, J. Sun, A nonsmooth version of Newton's method, Math. Programming 58 (1993) 353–368.
[25] A. Rösch, Error estimates for linear-quadratic control problems with control constraints, Opt. Methods Software 21 (1) (2006) 121–134.
[26] S. Schaffer, Higher order multi-grid methods, Math. Comput. 43 (1984) 89–115.
[27] V. Schulz, G. Wittum, Multigrid optimization methods for stationary parameter identification problems in groundwater flow, in: W. Hackbusch, G. Wittum (Eds.), Multigrid Methods V, Lecture Notes in Computational Science and Engineering, vol. 3, Springer, Berlin, 1998, pp. 276–288.
[28] E. Süli, Convergence of finite volume schemes for Poisson's equation on nonuniform meshes, SIAM J. Numer. Anal. 28 (1991) 1419–1430.
[29] U. Trottenberg, C. Oosterlee, A. Schüller, Multigrid, Academic Press, London, 2001.
[30] R. Wienands, C.W. Oosterlee, On three-grid Fourier analysis for multigrid, SIAM J. Sci. Comput. 23 (2001) 651–671.